Journal of Sound and Vibration (2002) **252**(4), 768–781
doi:10.1006/jsvi.2001.3990, available online at http://www.idealibrary.com on IDEAL®

A FOURIER SERIES METHOD FOR THE VIBRATIONS OF ELASTICALLY RESTRAINED PLATES ARBITRARILY LOADED WITH SPRINGS AND MASSES

W. L. Li and M. Daniels

United Technologies Carrier Corporation, A&R Building, Carrier Parkway, Syracuse, NY 13221, *U.S.A. E-mail: wen.li@carrier.utc.com*

(*Received* 26 *February* 2001, *and in final form* 6 *August* 2001)

1. INTRODUCTION

For plates simply supported along two opposite edges, an exact solution generally exists in the forms of trigonometric and hyperbolic functions [1]. However, the solution contains some integration and frequency constants that have to be determined from the boundary conditions. For an elastically restrained plate, these constants are functions of the stiffnesses of the boundary springs and can be numerically obtained by solving a non-linear equation. However, because of the number of involved variables (e.g., spring stiffnesses, plate aspect ratio and the Poisson ratio), it is obviously impractical to tabulate the numerical results as done for beams under various homogeneous boundary conditions. Consequently, one is essentially forced to repeat a normally tedious procedure to find the solutions on his own. As a matter of fact, probably due to the difficulty of such an approach, most existing investigations have involved some kinds of simplifications with respect to the arrangement or configuration of the elastic restraints [2–14].

Plates loaded with features like masses and springs are also a subject of extensive investigations [15–22]. Obviously, the loading condition will add another complicating factor to the plate problems that are already complicated enough in regard to the variety of boundary conditions. If an analytical method is employed, its complexity will usually increase with the number of attached features. Although the number and locations of the attachments may not be a significant complicating factor, theoretically, in the Rayleigh–Ritz method, they can still adversely affect the accuracy of the solution to a certain extent. This is because the mode shapes of a loaded plate tend to become more complicated, which makes it relatively difficult to select or construct appropriate trial functions.

For a plate that is simply supported or guided along each pair of opposite edges, its displacement solution is almost automatically sought as a double Fourier series. In that case, all the involved derivatives of the displacement can be directly obtained from the Fourier series through term-by-term differentiation and the Fourier coefficients are readily obtained from the governing differential equation. However, the Fourier series method is not widely used for other boundary conditions because of its potential convergence problem. Making use of the Stoke's transformation concept, Chung [23] extended the Fourier series method to the vibrations of circular cylinders under various homogeneous boundary conditions. This technique was later adopted by Lin and Wang [24] to study the

0022-460X/02/$35.00

vibrations of simply supported beams with rotational end restraints. Such an approach, however, is essentially only valid for beams under a boundary condition that prohibits the beams from moving at any end. Otherwise, it is more than likely that the Fourier series solution will face a convergence problem.

Simple polynomials have been used in combination with sinusoidal functions or Fourier series expansions to satisfy certain boundary conditions [25–29]. Li [30] recently proposed a simple and unified Fourier series method for beams with arbitrary boundary conditions by also expressing the beam displacement as a linear superposition of a Fourier series and an auxiliary polynomial. However, unlike in the previous investigations, there the polynomial function is used based on a totally different consideration, that is, regardless of boundary conditions, it is introduced to remedy any potential discontinuity problems associated with the original beam displacement and its related derivatives at the ends. Accordingly, the Fourier series will now represent a residual or conditioned beam displacement that is continuous and has at least three continuous derivatives everywhere. As a result, not only is it always possible to seek a solution in the form of a Fourier series for beams with any boundary conditions, but also the solution is drastically improved with respect to its accuracy and convergence. In this study, this technique will be extended to plates that are simply supported along a pair of opposite edges and elastically restrained along the others in a general manner. Moreover, the plates can be arbitrarily loaded with a number of masses and springs. The reliability and robustness of the current solution are demonstrated through numerical examples.

2. VIBRATION OF PLATES WITH ELASTIC RESTRAINTS ALONG EDGES

Figure 1 shows a rectangular plate simply supported along $y = 0$, b and elastically restrained along $x = 0$, a (for clarity, only the rotational and linear springs are shown here at $x = 0$ and a respectively). The plate may also be loaded with a number of springs and masses at arbitrary locations. The governing differential equation for the free vibration of the plate can be written as

$$\left(D\frac{\partial^4}{\partial x^4} + 2D\frac{\partial^4}{\partial x^2 \partial y^2} + D\frac{\partial^4}{\partial y^4} - \rho h\omega^2 + \sum_{i=1}^{N_K} \bar{k}_i \delta(x - x_i, y - y_i) - \omega^2 \sum_{i=1}^{N_m} \bar{m}_i \delta(x - x_i', y - y_i') \right) w(x, y) - \sum_{i=1}^{N_K} \bar{K}_i \frac{\partial \delta(x - \bar{x}_i, y - \bar{y}_i)}{\partial x} \frac{\partial w(\bar{x}_i, \bar{y}_i)}{\partial x} = 0, \quad (1)$$

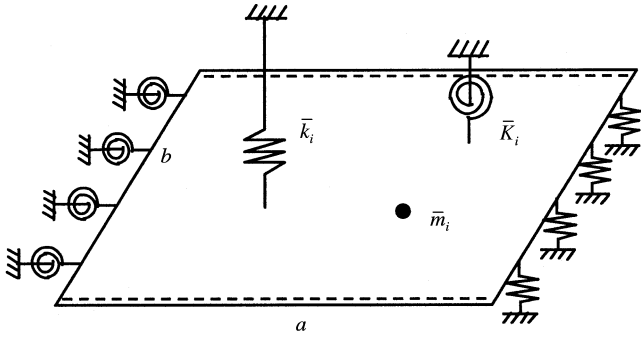

Figure 1. An elastically restrained plate arbitrarily loaded with springs and masses.

where $w(x, y)$ is the flexural displacement and ω is the angular frequency; D, ρ and h are, respectively, the flexural rigidity, the mass density and the thickness of the plate; $\bar{k}_i$ and $\bar{K}_i$ are the stiffnesses of the linear and rotational springs, respectively, located at (x_i, y_i) and (x_i', y_i') and $\bar{m}_i$ is the concentrated mass at $(\bar{x}_i, \bar{y}_i)$; and N_k, N_K and N_m are, respectively, the total numbers of the linear springs, rotational springs and masses attached to the plate. The last term on the left side of equation (1) is due to the moments about the y-axis applied by the rotational springs and can be derived by considering each of the moments as a pair of closely spaced forces of equal amplitude and opposite directions. The contribution of a moment about the x-axis can be taken into account in the same manner.

The boundary conditions along the elastically restrained edges can be expressed as

$$k_0 w = Q_x, \quad K_0 \partial w/\partial x = -M_x \qquad \text{along } x = 0 \tag{2, 3}$$

and

$$k_1 w = -Q_x, \quad K_1 \partial w/\partial x = M_x \qquad \text{along } x = a, \tag{4, 5}$$

where

$$M_x = -D\left(\frac{\partial^2 w}{\partial x^2} + \nu \frac{\partial^2 w}{\partial y^2}\right), \qquad Q_x = -D\left(\frac{\partial^3}{\partial x^3} + (2-\nu)\frac{\partial^3}{\partial x \partial y^2}\right), \tag{6, 7}$$

k_0 and k_1 are the linear stiffnesses, and K_0 and K_1 are the rotational stiffnesses of the elastic supports along $x = 0$ and a respectively. Equations (2)–(5) describe a general boundary condition from which all the familiar homogeneous boundary conditions (i.e., the various combinations of simply supported, clamped, free and guided) can be directly obtained by accordingly choosing the spring stiffness to be an extremely large or small number.

In the current investigation, a general solution to equations (1)–(5) will be sought in the form of a Fourier series. The convergence of a Fourier expansion has been fully studied in mathematics. An important theorem pertinent to this work states that [31]:

Let $f(x)$ be a continuous function of period $2a$ and have n derivatives, when $n-1$ derivatives are continuous and the nth derivative is absolutely integrable (the nth derivative may not exist at certain points). Then the coefficients of its Fourier expansion, $f(x) = \sum_{m=0}^{\infty} a_m \sin \lambda_{am} x$, $(\lambda_{am} = m\pi/a)$, satisfy that $\lim_{m\to\infty} a_m \lambda_{am}^n = 0$.

Mathematically, expanding $f(x)$, $x \in [0, a]$, into a Fourier sine series is equivalent to viewing it as part of periodic function which is simply $f(x)$ over $[0, a]$ and defined as $-f(x)$ over $(-a, 0)$. If $f(x)$ is continuous over $[0, a]$ and $f(0)$ and $f(a)$ are both identically zero, the Fourier sine series then simply represents a continuous function of period $2a$ and converges everywhere over the entire x-axis. However, when $f(0)$ (or $f(a)$) is not equal to zero, the Fourier sine series will still converge to zero at $x = 0$ (or $x = a$), regardless of the actual values of $f(0)$ (or $f(a)$). In such a case, the Fourier series only represents a piecewise continuous function. Therefore, the convergence of the Fourier series will become questionable according to the above theorem.

A remedy to this problem is proposed in reference [30] where a polynomial is introduced to take care of all the possible discontinuities with the original displacement function and its relevant derivatives at the endpoints. Accordingly, the Fourier series now simply represents a residual or conditioned displacement function that is periodic continuous and has at least

three continuous derivatives everywhere. Based on the same consideration, the solution for the current plate problem will be written as

$$w(x, y) = \sum_{m=0}^{\infty} [A_m \sin \lambda_{am} x + p(x)] \sin \lambda_{bn} y \quad \left(\lambda_{bn} = \frac{n\pi}{b}\right), \tag{8}$$

where $p(x)$ denotes a polynomial which will be determined below.

Because the potential discontinuity problem is only associated with the sine series expansions (of the displacement and its second derivative), the polynomial will be particularly introduced to satisfy

$$p(0) \sin \lambda_{bn} y = w(0, y) = \alpha_0 \sin \lambda_{bn} y, \qquad p(a) \sin \lambda_{bn} y = w(a, y) = \alpha_1 \sin \lambda_{bn} y, \tag{9, 10}$$

$$p''(0) \sin \lambda_{bn} y = \partial^2 w(0, y)/\partial x^2 = \beta_0 \sin \lambda_{bn} y, \qquad p''(a) \sin \lambda_{bn} y = \partial^2 w(a, y)/\partial x^2 = \beta_1 \sin \lambda_{bn} y. \tag{11, 12}$$

It is clear from equations (9)–(12) that unlike in the other techniques, the current polynomial is not used to ensure the satisfaction of any particular boundary condition. The displacement can also be expanded into a Fourier cosine series. In such a case, the polynomial will be used to deal with any possible discontinuities of the first and third derivatives (of the displacement) at the edges. Usually, a cosine series solution tends to converge faster than that in the form of equation (8) for a plate which is allowed to move along an edge. However, since the cosine series expansion has been adequately discussed in references [30, 32], the current study will be focused on the sine series solution.

Mathematically, the lowest order polynomial that satisfies equations (9)–(12) can be readily obtained as

$$p = \frac{\beta_1}{6a}(x^3 - a^2 x) - \frac{\beta_0}{6a}(2a^2 x - 3ax^2 + x^3) + \frac{\alpha_1 x}{a} + \frac{\alpha_0}{a}(a - x), \tag{13}$$

or, more concisely,

$$p = \boldsymbol{\zeta}(x)^{\mathrm{T}} \bar{\boldsymbol{\alpha}}, \tag{14}$$

where

$$\bar{\boldsymbol{\alpha}} = \{\alpha_0, \alpha_1, \beta_0, \beta_1\}^{\mathrm{T}} \tag{15}$$

and

$$\boldsymbol{\zeta}(x) = \{(a - x)/a \quad x/a \quad -(2a^2 x - 3ax^2 + x^3)/6a \quad (x^3 - a^2 x)/6a\}^{\mathrm{T}}. \tag{16}$$

Substitution of equations (8) and (13) into equations (2)–(7) results in

$$\hat{k}_0 \alpha_0 = -\left\{-\sum_{m=1}^{\infty} \lambda_{am}^3 A_m - \beta_0/a + \beta_1/a - (2 - \nu)\lambda_{bm}^2 \times \left(\sum_{m=1}^{\infty} \lambda_{am} A_m - \alpha_0/a + \alpha_1/a - \beta_0 a/3 - \beta_1 a/6\right)\right\}, \tag{17}$$

$$\hat{k}_1 \alpha_1 = \left\{-\sum_{m=1}^{\infty} (-1)^m \lambda_{am}^3 A_m - \beta_0/a + \beta_1/a - (2 - \nu)\lambda_{bn}^2 \times \left(\sum_{m=1}^{\infty} (-1)^m \lambda_{am} A_m - \alpha_0/a + \alpha_1/a + \beta_0 a/6 + \beta_1 a/3\right)\right\}, \tag{18}$$

$$\hat{K}_0\left(\sum_{m=1}^{\infty}\lambda_{am}A_m - \alpha_0/a + \alpha_1/a - \beta_0 a/3 - \beta_1 a/6\right) = \beta_0 - \nu\lambda_{bn}^2\alpha_0 \tag{19}$$

and

$$\hat{K}_1\left(\sum_{m=1}^{\infty}(-1)^m\lambda_{am}A_m - \alpha_0/a + \alpha_1/a + \beta_0 a/6 + \beta_1 a/3\right) = -\beta_1 + \nu\lambda_{bn}^2\alpha_1, \tag{20}$$

where $\hat{K}_i = K_i/D$ and $\hat{k}_i = k_i/D$ $(i = 0, 1)$.

From equations (17)–(20), the vector $\bar{\boldsymbol{\alpha}}$ can be determined as

$$\bar{\boldsymbol{\alpha}} = \sum_{m=0}^{\infty}\mathbf{H}_n^{-1}\mathbf{Q}_m^n A_m, \tag{21}$$

where

$$\mathbf{H}_n = \begin{bmatrix} \hat{k}_0 + (2-\nu)\lambda_{bn}^2/a & -(2-\nu)\lambda_{bn}^2/a & (2-\nu)\lambda_{bn}^2 a/3 - 1/a & (2-\nu)\lambda_{bn}^2 a/6 + 1/a \\ -(2-\nu)\lambda_{bn}^2/a & \hat{k}_1 + (2-\nu)\lambda_{bn}^2/a & (2-\nu)\lambda_{bn}^2 a/6 + 1/a & (2-\nu)\lambda_{bn}^2 a/3 - 1/a \\ \hat{K}_0/a - \nu\lambda_{bn}^2 & -\hat{K}_0/a & \hat{K}_0 a/3 + 1 & \hat{K}_0 a/6 \\ -\hat{K}_1/a & \hat{K}_1/a - \nu\lambda_{bn}^2 & \hat{K}_1 a/6 & \hat{K}_1 a/3 + 1 \end{bmatrix} \tag{22}$$

and

$$\mathbf{Q}_m^n = \{\lambda_{am}^3 + (2-\nu)\lambda_{bn}^2\lambda_{am}(-1)^{m+1}[\lambda_{am}^3 + (2-\nu)\lambda_{bn}^2\lambda_{am}] \;\; \hat{K}_0\lambda_{am} \; (-1)^{m+1}\hat{K}_1\lambda_{am}\}^{\mathrm{T}}. \tag{23}$$

Substituting equations (14) and (21) into equation (8), one immediately obtains

$$w(x, y) = \sum_{m=1}^{\infty} A_m[\sin\lambda_{am}x + \boldsymbol{\zeta}(x)^{\mathrm{T}}\mathbf{H}_n^{-1}\mathbf{Q}_m^n]\sin\lambda_{bn}y. \tag{24}$$

In order to be capable dealing with plates loaded with spring and/or masses, equation (24) needs to be modified as

$$w(x, y) = \sum_{m=1}^{\infty}\sum_{n=1}^{\infty} A_{mn}[\sin\lambda_{am}x + \boldsymbol{\zeta}(x)^{\mathrm{T}}\mathbf{H}_n^{-1}\mathbf{Q}_m^n]\sin\lambda_{bn}y. \tag{25}$$

Substituting equation (25) into equation (1) and following the Galerkin discretization procedure (that is, multiplying it with $(\sin\lambda_{am}x + \boldsymbol{\zeta}(x)^{\mathrm{T}}\mathbf{H}_n^{-1}\mathbf{Q}_m^n)\sin\lambda_{bn}y$ and integrating over the area of the plate), one will finally obtain

$$(\mathbf{K} - \omega^2\mathbf{M})\mathbf{A} = 0, \tag{26}$$

where

$$\mathbf{A} = \{A_{11}, A_{12}, A_{13}, \ldots, A_{i1}, A_{i2}, A_{i3}, \ldots, A_{M(N-1)}, A_{MN}\}^{\mathrm{T}},$$

$$\begin{aligned} K_{m'n',mn} = {} & D\{\delta_{m'm}\delta_{n'n}(\lambda_{am}^2 + \lambda_{bn}^2)^2 + \delta_{n'n}(\lambda_{bn}^4 S_{m'm}^n - 2\lambda_{bn}^2\hat{S}_{m'm}^n) + \delta_{n'n}S_{mm'}^n(\lambda_{am}^2 + \lambda_{bn}^2)^2 \\ & + \delta_{n'n}(\lambda_{bn}^4 Z_{m'n',mn} - 2\lambda_{bn}^2\hat{Z}_{m'n',mn})\} \\ & + 4/ab\sum_{i=1}^{N_k}\bar{k}_i(\sin\lambda_{am}x_i + \boldsymbol{\zeta}(x_i)^{\mathrm{T}}\mathbf{H}_n^{-1}\mathbf{Q}_m^n)(\sin\lambda_{am'}x_i + \boldsymbol{\zeta}(x_i)^{\mathrm{T}}\mathbf{H}_{n'}^{-1}\mathbf{Q}_{m'}^{n'}) \end{aligned}$$

$$\times \sin \lambda_{bn} y_i \sin \lambda_{bn'} y_i + 4/ab \sum_{i=1}^{N_K} \bar{K}_1 (\lambda_{am} \cos \lambda_{am} \bar{x}_i + (\partial \boldsymbol{\zeta}(\bar{x}_i)/\partial x)^{\mathrm{T}} \mathbf{H}_n^{-1} \mathbf{Q}_m^n)$$

$$\times (\lambda_{am'} \cos \lambda_{am'} \bar{x}_i + (\partial \boldsymbol{\zeta}(\bar{x}_i)/\partial x)^{\mathrm{T}} \mathbf{H}_{n'}^{-1} \mathbf{Q}_{m'}^{n'}) \sin \lambda_{bn'} \bar{y}_i \sin \lambda_{bn} \bar{y}_i \tag{27}$$

and

$$M_{m'n',mn} = \rho h \{\delta_{m'm} \delta_{n'n} + \delta_{n'n} (S_{m'm}^n + S_{mm'}^{n'} + Z_{m'n',mn})\}$$

$$+ 4/ab \sum_{i=1}^{N_m} \bar{m}_i (\sin \lambda_{am} x_i' + \boldsymbol{\zeta}(x_i')^{\mathrm{T}} \mathbf{H}_n^{-1} \mathbf{Q}_m^n)(\sin \lambda_{am'} x_i'$$

$$+ \boldsymbol{\zeta}(x_i')^{\mathrm{T}} \mathbf{H}_{n'}^{-1} \mathbf{Q}_{m'}^{n'}) \sin \lambda_{bn} y_i' \sin \lambda_{bn'} y_i', \tag{28}$$

with

$$S_{m'm}^n = \mathbf{P}_{m'}^{\mathrm{T}} \mathbf{H}_n^{-1} \mathbf{Q}_m^n, \qquad \hat{S}_{m'm}^n = \hat{\mathbf{P}}_{m'}^{\mathrm{T}} \mathbf{H}_n^{-1} \mathbf{Q}_m^n, \tag{29, 30}$$

$$Z_{mn,m'n'} = (\mathbf{H}_n^{-1} \mathbf{Q}_m^n)^{\mathrm{T}} \boldsymbol{\Xi} \mathbf{H}_{n'}^{-1} \mathbf{Q}_{m'}^{n'}, \qquad \hat{Z}_{mn,m'n'} = (\mathbf{H}_n^{-1} \mathbf{Q}_m^n)^{\mathrm{T}} \hat{\boldsymbol{\Xi}} \mathbf{H}_{n'}^{-1} \mathbf{Q}_{m'}^{n'}, \tag{31, 32}$$

$$\mathbf{P}_m = \frac{2}{a} \int_0^a \boldsymbol{\zeta}(x) \sin \lambda_{am} x \, \mathrm{d}x = \frac{2}{a} \left\{ \frac{1}{\lambda_{am}} \quad \frac{(-1)^{m+1}}{\lambda_{am}} \quad \frac{-1}{\lambda_{am}^3} \quad \frac{(-1)^m}{\lambda_{am}^3} \right\}^{\mathrm{T}}, \tag{33}$$

$$\hat{\mathbf{P}}_m = \frac{2}{a} \int_0^a \boldsymbol{\zeta}''(x) \sin \lambda_{am} x \, \mathrm{d}x = \frac{2}{a} \left\{ 0 \quad 0 \quad \frac{1}{\lambda_{am}} \quad \frac{(-1)^{m+1}}{\lambda_{am}} \right\}^{\mathrm{T}}, \tag{34}$$

$$\boldsymbol{\Xi} = 2/a \int_0^a \boldsymbol{\zeta}(x) \boldsymbol{\zeta}(x)^{\mathrm{T}} \, \mathrm{d}x$$

$$= \begin{bmatrix} 2/3 & 1/3 & -2a^2/45 & -7a^2/180 \\ 1/3 & 2/3 & -7a^2/180 & -2a^2/45 \\ -2a^2/45 & -7a^2/180 & 4a^4/945 & 31a^4/7560 \\ -7a^2/180 & -2a^2/45 & -31a^4/7560 & 4a^4/945 \end{bmatrix} \tag{35}$$

and

$$\hat{\boldsymbol{\Xi}} = 2/a \int_0^a \boldsymbol{\zeta}(x) (\mathrm{d}^2 \boldsymbol{\zeta}(x)/\mathrm{d}x^2)^{\mathrm{T}} \, \mathrm{d}x = \begin{bmatrix} 0 & 0 & 2/3 & 1/3 \\ 0 & 0 & 1/3 & 2/3 \\ 0 & 0 & -2a^2/45 & -7a^2/180 \\ 0 & 0 & -7a^2/180 & -2a^2/45 \end{bmatrix}. \tag{36}$$

In equation (26), it has been assumed that the summations over m and n are truncated to the first M and N terms respectively. Obviously, the natural frequencies and eigenvectors can now be easily obtained by solving a standard matrix eigenproblem. Since the components of each eigenvector are actually the expansion coefficients of the Fourier series, the corresponding mode shape can be directly determined from equation (25). Finally, the normalized mode shape, satisfying

$$\int_0^a \int_0^b w^2 \, \mathrm{d}x \, \mathrm{d}y = 1, \tag{37}$$

can be expressed as

$$\psi(x, y) = \sum_{m=1}^{M} \sum_{n=1}^{N} \bar{A}_{mn}[\sin \lambda_{am} x + \boldsymbol{\zeta}(x)^{\mathrm{T}} \mathbf{H}_n^{-1} \mathbf{Q}_m^n] \sin \lambda_{bn} y, \tag{38}$$

where

$$\bar{A}_{mn} = A_{mn}/\chi \tag{39}$$

and

$$\chi = \frac{\sqrt{ab}}{2} \left(\sum_{m,n,m'=1} (\delta_{mm'} + 2S_{mm'}^n + Z_{mn,m'n}) A_{mn} A_{m'n} \right)^{1/2}. \tag{40}$$

Again, it must be emphasized that the objective of introducing the polynomial is to improve the accuracy and convergence of the Fourier series solution. The results will be demonstrated below through numerical examples.

3. RESULTS AND DISCUSSIONS

First, let us consider a square plate that is clamped along $x = 0$ and a. The clamped boundary condition can be easily generated by simply setting the stiffnesses of the four springs equal to infinity (which is represented by a very large number, 10^{10}, in the following calculations). The characteristic equation for a C–S–C–S plate is well known as [1]

$$2\lambda_1\lambda_2(\cos \lambda_1 \cosh \lambda_2 - 1) + (\lambda_1^2 - \lambda_2^2)\sin \lambda_1 \sinh \lambda_2 = 0, \tag{41}$$

where

$$\Omega = b^2\omega(\rho h/D)^{1/2}, \qquad \lambda_{1,2} = (a/b)(\Omega \mp n^2\pi^2)^{1/2}. \tag{42, 43}$$

Table 1 shows the first six frequency parameters $\Omega_{mn} = \omega_{mn}a^2\sqrt{\rho h/D}$ estimated by using different numbers of terms in equation (24). The second subscript n of the frequency parameter Ω_{mn} indicates the number of half-sine waves in the y direction for the corresponding mode and the first subscript m denotes the mth lowest mode for the given index n. The results calculated from equation (41) are also presented in Table 1 for comparison. It is seen that the current method has led to an excellent prediction even by using a small number of terms.

The next example also deals with a familiar boundary condition: simply supported along $x = 0$ and free along $x = a$. This boundary condition is readily represented by setting

TABLE 1

Frequency parameters, $\Omega = \omega a^2\sqrt{\rho h/D}$, for a C–S–C–S square plate

	$\Omega_{mn} = \omega_{mn}a^2\sqrt{\rho h/D}$					
Solution	Ω_{11}	Ω_{12}	Ω_{21}	Ω_{22}	Ω_{13}	Ω_{31}
Current, $M = 5$	28·9514	54·7498	69·3275	94·6142	102·239	129·099
Current, $M = 10$	28·9509	54·7438	69·3271	94·5866	102·219	129·096
Current, $M = 20$	28·9509	54·7431	69·3270	94·5853	102·216	129·096
Equation (41)	28·9509	54·7431	69·3270	94·5853	102·216	129·096

TABLE 2

Frequency parameters, $\Omega = \omega a^2\sqrt{\rho h/D}$, for an S–S–F–S square plate

	$\Omega_{mn} = \omega_{mn}a^2\sqrt{\rho h/D}$					
Solution	Ω_{11}	Ω_{21}	Ω_{12}	Ω_{22}	Ω_{31}	Ω_{13}
Current, $M = 5$	11·6859	27·7971	41·2308	59·2435	62·3701	90·5177
Current, $M = 10$	11·6846	27·7581	41·1985	59·0756	61·8838	90·3108
Current, $M = 20$	11·6845	27·7564	41·1967	59·0659	61·8615	90·2948
Equation (44)	11·6845	27·7564	41·1967	59·0655	61·8606	90·2941

TABLE 3

The frequency parameters, $\Omega^2 = \omega^2 a^4 \rho h/\pi^4 D$, for an S–S–S–S square plate with rotational restraints along $x = 0$ and a $M = 10$

	$\Omega_{mn}^2 = \omega_{mn}^2 a^4 \rho h/\pi^4 D$			
$\hat{K}_0 = \hat{K}_1 a$	Ω_{11}^2	Ω_{21}^2	Ω_{31}^2	Ω_{41}^2
0	4·0	25·0	100·0	289·0
10	6·16826	34·8307	124·569	335·975
100	8·14370	46·2673	160·131	417·339
∞	8·60448	49·3408	171·089	445·823

$\hat{k}_0 a^3 = \infty$ and $\hat{K}_0 = \hat{K}_1 = \hat{k}_1 = 0$. The corresponding frequency parameters can be determined from

$$\lambda_2(\Omega - (1-\nu)n^2\pi^2)^2 \sin\lambda_1 \cosh\lambda_2 - \lambda_1(\Omega + (1-\nu)n^2\pi^2)^2 \cos\lambda_1 \sinh\lambda_2 = 0. \quad (44)$$

In Table 2, the six lowest frequency parameters obtained from the use of different numbers of terms in the Fourier expansion are given. Again, the current solution shows an excellent agreement with the classical solution, equation (44).

A remarkable convergence of the solution has been observed in both examples, which is perhaps the most important characteristic of the current technique. Theoretically, because of the existence of the free edge, the second example represents a more challenging case for checking the convergence of a Fourier series solution.

Now, consider a plate elastically restrained against rotations along the edges $x = 0$ and a. The four lowest frequency parameters, $\Omega = \omega a^2\sqrt{\rho h/D}$, calculated by using only 10 terms are listed in Table 3 for different spring stiffnesses. For $\hat{K}_0 a = \hat{K}_1 a = 0$ and $\hat{K}_0 a = \hat{K}_1 a = \infty$, the boundary conditions at both edges will degenerated to the familiar simply supported and clamped cases respectively. To understand the effects of the (rotational) stiffness on the modes, the mode shapes sliced at $y = b/2$ are plotted in Figures 2–5. It is seen that as the stiffness increases, the slopes towards the edges become less steep which agrees with intuition. In Table 4, the calculated fundamental frequencies are compared with the previous results for various combinations of the plate aspect ratio and spring stiffness.

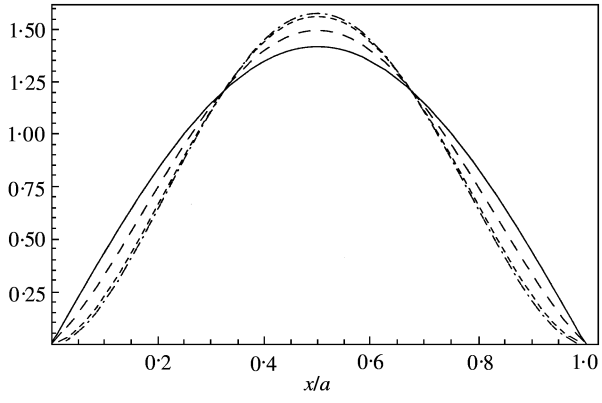

Figure 2. Modes corresponding to Ω_{11} for different stiffness values: ——, $\hat{K}_0 a = 0$; – – –, $\hat{K}_0 a = 10$; - - - -, $\hat{K}_0 a = 100$; – · –, $\hat{K}_0 a = \infty$.

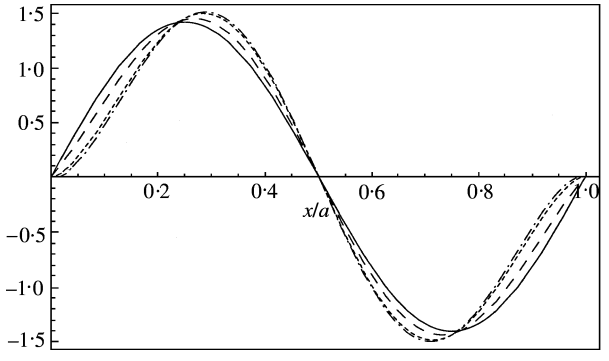

Figure 3. Modes corresponding to Ω_{21} for different stiffness values: ——, $\hat{K}_0 a = 0$; – – –, $\hat{K}_0 a = 10$; - - - -, $\hat{K}_0 a = 100$; – · –, $\hat{K}_0 a = \infty$.

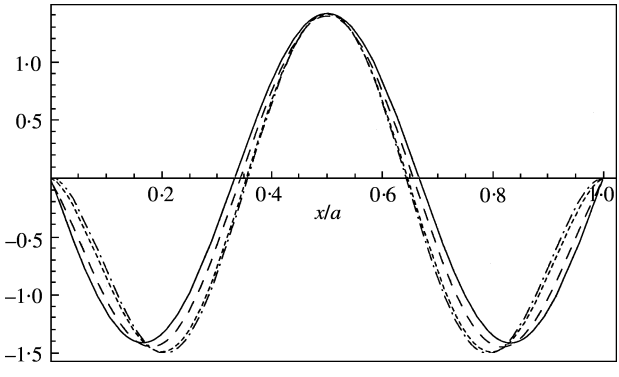

Figure 4. Modes corresponding to Ω_{31} for different stiffness values: ——, $\hat{K}_0 a = 0$; – – –, $\hat{K}_0 a = 10$; - - - -, $\hat{K}_0 a = 100$; – · –, $\hat{K}_0 a = \infty$.

To further examine the accuracy and convergence of the solution, a more complicated problem will be considered here: a square plate clamped along $x = 0$ and elastically restrained by two independent (rotational and translational) springs along $x = a$. After

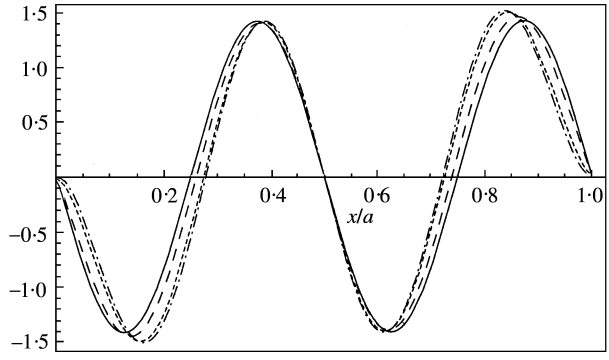

Figure 5. Modes corresponding to Ω_{41} for different stiffness values: ——, $\hat{K}_0 a = 0$; – – –, $\hat{K}_0 a = 10$; - - - -, $\hat{K}_0 a = 100$; – · –, $\hat{K}_0 a = \infty$.

TABLE 4

The fundamental frequencies, $\Omega^2 = \omega^2 a^2 b^2 \rho h/\pi^4 D$, for S–S–S–S plates with different aspect ratios and rotational stiffnesses. $M = 10$

	$\Omega^2 = \omega^2 a^2 b^2 \rho h/\pi^4 D$					
	$b/a = 0{\cdot}5$		$b/a = 1{\cdot}0$		$b/a = 1{\cdot}5$	
$\hat{K}_0 a = \hat{K}_1 a$	Current	Reference [1]†	Current	Reference [1]	Current	Reference [1]
0	6·25	6·25	4·0	4·0	4·694	4·694
1	6·345	6·333	4·373	4·373	5·530	5·530
10	6·847	6·837	6·168	6·169	9·446	9·444
100	7·514	7·519	8·144	8·137	13·557	—
∞	7·691	7·692	8·604	8·593	14·487	—

†See pp. 120–121.

TABLE 5

Frequency parameters, $\Omega = \omega a^2 \sqrt{\rho h/D}$, for a C–S–E–S square plate, $\hat{k}_1 a^3 = 100$ and $\hat{K}_1 a = 10$

	$\Omega_{mn} = \omega_{mn} a^2 \sqrt{\rho h/D}$					
Solution	Ω_{11}	Ω_{21}	Ω_{12}	Ω_{22}	Ω_{31}	Ω_{13}
Current, $M = 5$	19·4025	40·7803	44·8252	67·1697	81·6234	92·5912
Current, $M = 10$	19·3985	40·7213	44·8115	67·0473	81·0794	92·5271
Current, $M = 20$	19·3982	40·7187	44·8104	67·0424	81·0525	92·5217
Equation (45)	19·3982	40·7187	44·8104	67·0422	81·0514	92·5214

lengthy, but straightforward, mathematical manipulations, the characteristic equation can be obtained as

$$\lambda_1\lambda_2(\Omega^2 - n^4\pi^4(1-\nu)^2 + b^4\hat{k}\hat{K}) + \lambda_1\lambda_2(\Omega^2 + n^4\pi^4(1-\nu)^2 - b^4\hat{k}\hat{K})\cos\lambda_1\cosh\lambda_2$$

$$+ (n\pi/\sigma)^2(\Omega^2(1-2\nu) - n^4\pi^4(1-\nu)^2 + b^4\hat{k}\hat{K})\sin\lambda_1\sinh\lambda_2$$

TABLE 6

Fundamental frequencies, $\Omega = \omega a^2\sqrt{\rho h/D}$, for a C–S–E–S square plate with various combinations of the rotational and translational springs at $x = a$ $M = 20$

	$\Omega = \omega a^2\sqrt{\rho h/D}$			
$\hat{K}_1 a$	$\hat{k}_1 a^3 = 0$	$\hat{k}_1 a^3 = 10$	$\hat{k}_1 a^3 = 100$	$\hat{k}_1 a^3 = \infty$
0	12·6874	13·9315	19·2195	23·6463
10	13·4098	14·3460	19·3982	26·5556
100	13·6491	14·4891	19·4782	28·5523
∞	13·6858	14·5114	19·4917	28·9509

TABLE 7

Frequency parameters, $\Omega = \omega a^2\sqrt{\rho h/D}$, for a C–S–E–S square plate with $\hat{k}_1 a^3 = 10$ and $\hat{K}_1 a = 0$. $M = N = 10$

	$\Omega = \omega a^2\sqrt{\rho h/D}$					
Modes	1	2	3	4	5	6
Simple plate	13·9316	33·6801	42·0911	63·3111	72·7221	90·8136
Loaded plate	14·6956	36·6446	42·0911	63·3111	69·7717	79·9377

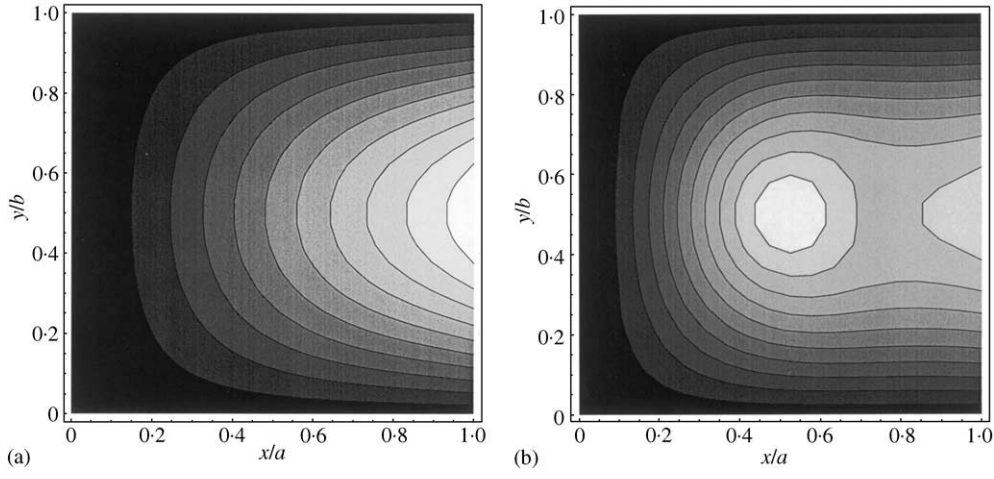

Figure 6. The first mode of the plate: (a) unloaded; (b) loaded.

$$+ \lambda_1\Omega\sigma^2(\lambda_2^2\hat{K}a - \hat{k}a^3)\cos\lambda_1\sinh\lambda_2$$
$$+ \lambda_2\Omega\sigma^2(\lambda_1^2\hat{K}a + \hat{k}a^3)\sin\lambda_1\cosh\lambda_2 = 0, \tag{45}$$

where $\sigma = b/a$.

For $\hat{k}_1 a^3 = 100$ and $\hat{K}_1 a = 10$, the frequency parameters estimated by using different numbers of terms are given in Table 5 together with those calculated from equation (45).

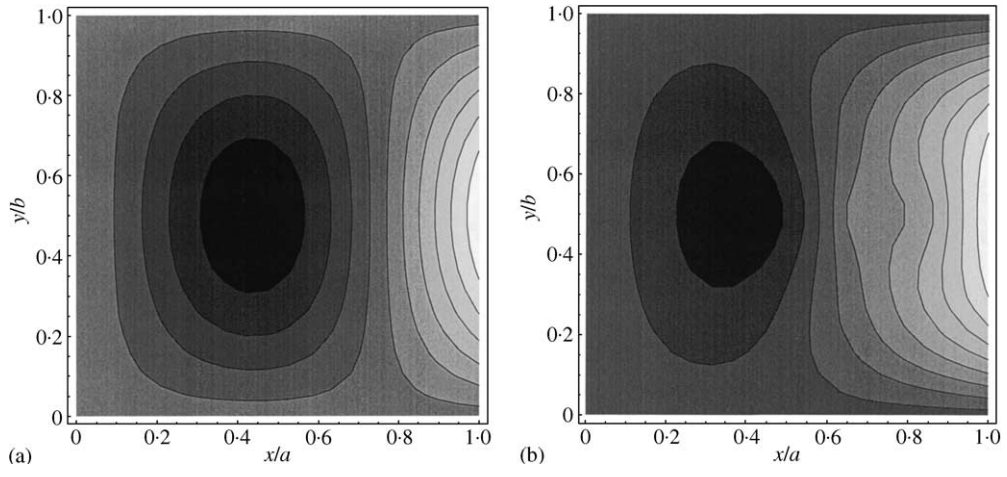

Figure 7. The second mode of the plate: (a) unloaded; (b) loaded.

The excellent accuracy and convergence of the current solution are again demonstrated. The fundamental frequencies are shown in Table 6 for various combinations of the spring stiffnesses.

Let us now assume in the last problem that $\hat{k}_1 a^3 = 10$ and $\hat{K}_1 a = 0$, and the plate carries a concentrated mass, $\bar{m}_1/\rho h a^2 = 0{\cdot}5$, at its center. In addition, the plate is reinforced at $(3a/4, a/2)$ by a structure which is represented by a translational stiffness, $\bar{k}_1 a^2/D = 100$, and a rotational stiffness, $\bar{K}_1/D = 100$. In Table 7, several lowest frequency parameters are presented for this plate and its unloaded counterpart as well. As expected, the third and fourth modes are not affected by the addition of the mass and springs because they all happen to fall on the nodal lines. The first two modes of the loaded and unloaded plates are compared in Figures 6 and 7. A total of 100 terms, $M = N = 10$, is used in this calculation.

4. CONCLUSIONS

A simple and unified method has been described for the vibration analysis of plates that are simply supported along two opposite edges and elastically restrained along the others in an arbitrary manner. The plate displacement is expressed as the combination of a Fourier sine series and an auxiliary polynomial. The polynomial is introduced to take care of all the possible discontinuities associated with the original displacement function and its relevant derivatives at boundaries so that the Fourier series now simply represents a conditioned displacement function with at least three continuous derivatives. As a result, the accuracy and convergence of the Fourier series solution can be drastically improved as repeatedly demonstrated by the numerical examples.

REFERENCES

1. A. W. Leissa 1993 *Vibration of Plates*. Acoustical Society of America.
2. T. E. Carmichael 1959 *Quarterly Journal of Mechanics and Applied Mathematics* **12**, 29–42. The vibration of a rectangular plate with edges elastically restrained against rotation.

3. A. W. LEISSA, P. A. A. LAURA and R. H. GUTIERREZ 1980 *Journal of Applied Mechanics* **47**, 891–895. Vibrations of rectangular plates with non-uniform elastic edge supports.
4. P. A. A. LAURA and R. O. GROSSI 1978 *Journal of Sound and Vibration* **59**, 355–368. Transverse vibration of a rectangular plate elastically restrained against rotation along three edges and free on the fourth edge.
5. P. A. A. LAURA and R. O. GROSSI 1981 *Journal of Sound and Vibration* **75**, 101–107. Transverse vibrations of rectangular plates elastically restrained against translation and rotation.
6. P. A. A. LAURA, L. E. LUISONI and C. P. FILIPICH 1997 *Journal of Sound and Vibration* **55**, 327–333. A note on the determination of the fundamental frequency of vibration of thin rectangular plates with edges possessing different rotational flexibility coefficients.
7. G. B. WARBURTON and S. L. EDNEY 1984 *Journal of Sound and Vibration* **95**, 537–552. Vibrations of rectangular plates with elastically restrained edges.
8. M. MUKHOPADHYAY 1979 *Journal of Sound and Vibration* **67**, 459–468. Free vibrations of rectangular plates with edges having different degrees of rotational restraint.
9. D. J. GORMAN 1980 *Journal of Applied Mechanics* **56**, 893–899. A comprehensive study of the free vibration of rectangular plates resting on symmetrically-distributed uniform elastic edge supports.
10. A. BERRY 1994 *Journal of the Acoustical Society of America* **96**, 889–901. A new formulation for vibrations and sound radiation of fluid-loaded plates with elastic boundary conditions.
11. A. V. BAPAT, N. VENKATRAMANI and S. SURYANARAYAN 1998 *Journal of Sound and Vibration* **120**, 127–140. Simulation of classical edge conditions by finite elastic restraints in the vibration analysis of plates.
12. K. N. SAHA, R. C. KAR and P. K. DATTA 1996 *Journal of Sound and Vibration* **192**, 885–904. Free vibration analysis of rectangular Mindlin plate with elastic restraints uniformly distributed along the edges.
13. K. H. KANG and K. J. KIM 1996 *Journal of Sound and Vibration* **190**, 207–220. Modal properties of beams and plates on resilient supports with rotational and translational complex stiffness.
14. Y. XIANG, K. M. LIEW and S. KITIPORNCHAI 1997 *Journal of Sound and Vibration* **204**, 1–16. Vibration analysis of rectangular Mindlin plate resting on elastic edge supports.
15. H. COHEN and F. HANDELMAN 1956 *Journal of Franklin Institute* **261**, 319–329. Vibrations of a rectangular plate with distributed added mass.
16. C. L. AMBA-RAO 1964 *Journal of Applied Mechanics* **31**, 500–551. On the vibration of a rectangular plate carrying a concentrated mass.
17. Y. C. DAS and D. R. NAVARATNA 1963 *Journal of Applied Mechanics* **30**, 31–36. Vibrations of a rectangular plate with concentrated mass, spring, and dashpot.
18. W. F. STOKEY and C. F. ZOROWSKI 1959 *Journal of Applied Mechanics* **26**, 210–216. Normal vibrations of a uniform plate carrying any number of finite masses.
19. J. S. WU and S. S. LUO 1997 *Journal of Sound and Vibration* **200**, 179–194. Use of the analytical-and-numerical-combined method in the free vibration analysis of a rectangular plate with any number of point masses and translational springs.
20. W. L. LI and H. J. GIBELING 1999 *Journal of Sound and Vibration* **220**, 117–133. Acoustic radiation from a rectangular plate reinforced by finite springs at arbitrary locations.
21. L. A. BERGMAN, J. K. HALL, G. G. G. LUESCHEN and D. M. MCFARLAND 1993 *Journal of Sound and Vibration* **162**, 281–310. Dynamic Green's functions for Levy plates.
22. M. S. INGBER, A. L. PATE and J. M. SALAZAR 1992 *Journal of Sound and Vibration* **153**, 143–166. Vibration of a clamped plate with concentrated mass and spring attachments.
23. H. CHUNG 1981 *Journal of Sound and Vibration* **196**, 285–293. Free vibration analysis of circular cylindrical shells.
24. J. T.-S. WANG and C.-C. LIN 1996 *Journal of Sound and Vibration* **196**, 285–293. Dynamic analysis of generally supported beams using Fourier series.
25. D. ZHOU 1996 *Journal of Sound and Vibration* **189**, 81–88. Natural frequencies of rectangular plates using a set of static beam functions in the Rayleigh–Ritz method.
26. D. ZHOU 1995 *Computers and Structures* **57**, 731–735. Natural frequencies of elastically restrained rectangular plates using a set of static beam functions in the Rayleigh–Ritz method.
27. E. E. LUNDQUIST and E. STOWELL 1942 (*NACA report* 733.) Critical compressive stress for flat rectangular plates supported along all edges and elastically restrained against rotations along the unloaded edges. (Its review is available in reference [1], pp. 118–119.)
28. W. K. TSO 1996 *Journal of the American Institute of Aeronautics and Astronautics* **4**, 733–735. On the fundamental frequency of a four point-supported square elastic plate.

29. C. P. FILIPICH and M. B. ROSALES 2000 *Journal of Sound and Vibration* **230**, 521–539. Arbitrary precision frequencies of a free rectangular thin plate.
30. W. L. LI 2000 *Journal of Sound and Vibration* **237**, 709–725. Free vibrations of beams with general boundary conditions.
31. G. P. TOLSTOV 1965 *Fourier Series*. Englewood Cliffs, NJ: Prentice-Hall.
32. W. L. LI 2001 *Journal of Sound and Vibration* **246**, 751–756. Dynamic analysis of beams with arbitrary elastic supports at both ends.